Combined local current distribution measurements and high resolution neutron radiography of operating Direct Methanol Fuel Cells

Alexander Schröder [a, *], Klaus Wippermann [a], Jürgen Mergel [a], Werner Lehnert [a], Detlef Stolten [a], Tilman Sanders [b], Thorsten Baumhöfer [b], Dirk U. Sauer [b], Ingo Manke [c, d], Nikolay Kardjilov [d], André Hilger [d], Jana Schloesser [d], John Banhart [c, d], Christoph Hartnig [e]

[a] Institute of Energy Research, IEF-3: Fuel Cells, Forschungszentrum Jülich GmbH, 52425 Jülich, Germany
[b] Institute for Power Electronics and Electrical Drives (ISEA), RWTH Aachen University, Jägerstraße 17–19, 52066 Aachen, Germany
[c] Institute of Materials Science and Technology, Berlin Institute of Technology, Hardenbergstraße 36, 10623 Berlin, Germany
[d] Helmholtz Centre Berlin (Hahn-Meitner-Institute), SF3, Glienicker Straße 100, 14109 Berlin, Germany
[e] Centre for Solar Energy and Hydrogen Research (ZSW), Helmholtzstraße 8, 89081 Ulm, Germany
present address: BASF Fuel Cell GmbH, Industriepark Höchst, 65926 Frankfurt/Main

Abstract

The current and fluid distribution in Direct Methanol Fuel Cells (DMFCs) was investigated *in situ* by means of combined high resolution neutron radiography and locally resolved current distribution measurements. The used neutron radiography set-up allows high spatial resolutions down to 70 µm at the full test cell area. A local formation of water droplets in the cathode flow field channels could be observed. Strongly inhomogeneous current distributions during cathodic flooding processes result in a performance loss of up to 30 % of the initial value. Single CO_2 bubbles can be observed at low current densities. The water and current distribution during bi-functional operation of a DMFC was measured for the first time.

Keywords: DMFC, high resolution neutron radiography, current distribution, fluid distribution

* Corresponding author. Tel.: +49 2461 61-1579; fax: +49 61-6695.
E-mail address: a.schroeder@fz-juelich.de (A. Schröder).

1. Introduction

One of the main problems in the development of Direct Methanol Fuel Cells is the uneven fluid distribution. While CO_2 bubbles may inhibit the methanol supply on the anode side, water droplets on the cathode side block the oxygen supply. Combined with the concentration decrease of the reactants across the active area along the flow field channels, these effects lead to a pronounced inhomogeneous current distribution as well as to a power loss of the fuel cell. With the knowledge of the local distribution and transport behaviour of CO_2 bubbles and water droplets at different operation modes, investigations on the improvement of cell components and design are possible.

By means of segmented circuit boards, the currents of separate cell segments can be measured during operation of the cell. In order to investigate the effects leading to the inhomogeneous current distribution, a further measurement technique is mandatory, allowing the observation of the CO_2 and water distribution. Several authors used cells with a transparent cover to observe the carbon dioxide evolution and the two phase flow behaviour visually [1]–[4]. An alternative method is synchrotron X-ray radiography [5], [6]. In order to use a completely non invasive method for the observation of CO_2 and water, we used neutron radiography which has been proven its applicability for a variety of questions [7]–[10]. Neutron radiation has a high attenuation coefficient for hydrogen compared to the one of most metals. The neutron beam is less affected by the solid cell components compared to liquid water which leads to a strong absorption of the beam. Thus, the distribution of hydrogen-rich species can be observed during operation. In the test set-up, the neutron radiation is attenuated while passing the cell in through-plane direction. The transmitted radiation is converted into visible light by means of a scintillator which then can be detected by a charge-coupled device camera. Placing the scintillator closely to the test cell allows for resolutions down to 70 µm. A combination of

neutron radiography and segmented current distribution measurement results in an *in situ* correlation of the current and fluid distribution.

2. Experimental

2.1 Electrochemical set-up and test cell

The functional layers of the used membrane electrode assemblies (MEAs) with an active area of 4.2×4.2 cm^2 were prepared onto carbon cloth (Ballard). The microporous layer consisted of 60 wt.% carbon (Cabot) and 40 wt.% PTFE. The anode catalyst consisted of 75 wt.% Pt/Ru and 25 % carbon (Johnson Matthey). The Pt/Ru loading of the anodes was 2 mg cm^{-2}. The cathode catalyst had a composition of 57 wt.% Pt and 43 % carbon (Johnson Matthey) with a Pt loading of 2 mg cm^{-2}. The anode and cathode electrodes were hot-pressed on both sides of a Nafion N-115 membrane.

Two types of graphite flow fields were used: The first flow field consists of a grid structure with ribs (1×1 mm^2 area) and channels (1 mm width and depth). The second flow field consists of a twofold meander with separate supply of both channels. The flow arrangement of both flow field geometries was counter flow. The air feed was at the top and the methanol feed at the bottom of the cell.

All measurements were carried out at a temperature of 70 °C and ambient pressure. The anode was constantly fed by a methanol solution with a concentration of 1 mol l^{-1} and a flow rate of either 2.19 ml min^{-1} or 2.56 ml min^{-1}. The cathode was supplied with an air flow of either 378 ml min^{-1} or 20 ml min^{-1}. The respective values, depending on the operation modes, are indicated in the figures below.

The current distribution was measured with a setup as described in [11]. Adapted to the flow field geometries, circuit boards with 25 and 28 segments were used.

2.2 Neutron radiography

The radiography experiments were performed at the neutron tomography instrument CONRAD/V7 at Helmholtz Centre Berlin (formerly Hahn-Meitner Institute) in Germany. The imaging set-up is based on a pinhole geometry with a small variable aperture. The main part of the detector system is a 16-bit low-noise CCD camera (Andor DW436N with 2048×2048 pixel^2) [12]. The camera is focused by a lens system on a neutron sensitive scintillator screen (Gadox) which was mounted close to the fuel cells to ensure high spatial resolutions down to 70 µm.

3. Results

3.1 Observation of flooding effects

Under the chosen conditions, a flooding effect on the cathode side within the grid flow field channels has been observed. Before starting the measurement, the anode side was filled with methanol solution and the cathode side was completely filled with air. Initially, the current load was set to 300 mA cm^{-2} and water droplets began to form homogeneously in the bottom part of the flow field. During the ten-second exposure time of the first radiography, (Fig. 1a), the droplets were still small, allowing a sufficient oxygen supply, resulting in a homogeneous current distribution ($I_{max}/I_{min} = 1.7$, Fig. 1b) and a high power density ($p = 113$ mW cm^{-2}). Growing bigger, the droplets blocked the oxygen supply significantly (Fig. 1c). The current distribution was highly inhomogeneous ($I_{max}/I_{min} = 6.3$, Fig. 1d) and the power density attained its minimum ($p = 78$ mW cm^{-2}). The spontaneous discharge of water partially reversed the flooding effect only 12 seconds later ($I_{max}/I_{min} = 2.3$, $p = 100$ mW cm^{-2}, Fig. 1e, f). Leaving the channels irregularly at different areas, the water droplets led to a reduced water content of the cathode flow field and therewith to more homogeneous

4

conditions. 471 seconds after the start of the measurement, the current distribution and power density nearly achieved their initial values ($I_{max}/I_{min} = 1.8$, p = 110 mW cm^{-2}, Fig. 1g, h).

At the same operation conditions, the average velocity of air inside the channels of the twofold meander flow field is significantly higher so that no large water amounts could build up and therefore no flooding effect occurred.

3.2 Water and gas distribution in dependence on current density

Test cells with both flow field geometries were investigated with three different average current densities applying constant flow rates. The grid structure allows the observation of CO_2 bubbles on the anode side at low current densities. The gas evolution rate at 50 mA cm^{-2} is small enough that most of the CO_2 bubbles hardly move during exposure time (Fig. 2a). On the cathode side, there is no visible water content. At 150 mA cm^{-2}, according to the current density, the CO_2 and water evolution rate is higher (Fig. 2c). Single CO_2 bubbles cannot be observed as they move faster and the temporal resolution is too low. The formation of liquid water occurs in the lower part of the flow field. At 300 mA cm^{-2}, the CO_2 evolution is further increased and the formation of liquid water expands to about two thirds of the flow field area (Fig. 2e).

The results concerning the measurements with the twofold meander test cell are similar. With increasing current density, both the water and the CO_2 formation grow (Fig. 2b, d, f). As the average velocity of the fluids in the channels is much higher than in case of the grid flow field, even at a low current density of 50 mA cm^{-2}, single CO_2 bubbles are not observable. At medium and high current density, only small water droplets can be observed as a result of the high air velocity [13].

3.3 Water and current distribution during bi-functional operation

Several studies of Direct Methanol Fuel Cells (see e.g. [14]) have shown that at low air flow rates and current densities, the active cell area is split up in two domains: The domain close to the inlet of the oxygen channel operates in normal fuel cell mode (galvanic domain). The domain close to the outlet of the oxygen channel works in electrolysis mode: The current produced in the galvanic domain is consumed to convert methanol to hydrogen (electrolytic domain).

In the cathode flow fields of our square-shaped test cells, the air flows from the top to the bottom of the cell. At conditions of bi-functional operation, a galvanic domain is expected at the top of the cell and an electrolytic domain at the bottom of the cell. This is confirmed by synchronous current distribution measurements and neutron radiography for the different cathode flow field geometries, i.e. grid flow field (Fig. 3a, b) and twofold meander flow field (Fig. 3c, d). Fig. 3a and c depict the water/gas distribution while Fig. 3b and d show the colour map of the respective current distribution. Independent of the flow field geometry, a negative (electrolytic) current results in the bottom part of the cells (green colour), while a positive (galvanic) one is observed in the upper part of the cells. Since formation of water only takes place in the galvanic regime water droplets in the cathode flow field channels emerge only in the top part of both cells (dark spots). The channels in the bottom part of the cells appear light because no water droplets are formed in the cathode channels and hydrogen gas is evolved in the anode channels. This combined approach represents to our knowledge the first direct visualization of water and gas distribution during bi-functional DMFC operation.

4. Conclusions

The method of high resolution neutron radiography provides a detailed insight into the changing water and gas distribution in Direct Methanol Fuel Cells under different operating conditions. The used set-up allows for high spatial resolutions down to 70 µm. As *in situ* method, neutron radiography is especially valuable in combination with a simultaneous measurement of the local current distribution, because it allows the correlation of liquid water and carbon dioxide formation and current distribution. The study of this interdependency offers the possibility to optimize the water management and performance of Direct Methanol Fuel Cells respecting a homogeneous water, carbon dioxide and current distribution.

Acknowledgements

References

[1] C. W. Wong, T. S. Zhao, Q. Ye, J. G. Liu, Journal of The Electrochemical Society 152 (2005) A1600–A1605

[2] P. Argyropoulos, K. Scott, W. M. Taama, Electrochimica Acta 44 (1999) 3575–3584

[3] H. Yang, T. S. Zhao, Q. Ye, Journal of Power Sources 139 (2005) 79–90

[4] Q. Liao, X. Zhu, X. Zheng, Y. Ding, Journal of Power Sources 171 (2007) 644–651

[5] C. Hartnig, I. Manke, R. Kuhn, N. Kardjilov, J. Banhart, W. Lehnert, Applied Physics Letters 92, 134106 (2008)

[6]   I. Manke, C. Hartnig, M. Grünerbel, W. Lehnert, N. Kardjilov, A. Haibel, A. Hilger, J. Banhart, H. Riesemeier, Applied Physics Letters 90, 174105 (2007)

[7]   D. Kramer, E. Lehmann, G. Frei, P. Vontobel, A. Wokaun, G. G. Scherer, Nuclear Instruments and Methods in Physics Research A 542 (2005) 52–60

[8]   C. Hartnig, I. Manke, N. Kardjilov, A. Hilger, M. Grünerbel, J. Kaczerowski, J. Banhart, W. Lehnert, Journal of Power Sources 176 (2008) 452–459

[9]   I. Manke, C. Hartnig, M. Grünerbel, J. Kaczerowski, W. Lehnert, N. Kardjilov, A. Hilger, J. Banhart, W. Treimer, M. Strobl, Applied Physics Letters 90, 184101 (2007)

[10] I. Manke, C. Hartnig, N. Kardjilov, M. Messerschmidt, A. Hilger, M. Strobl, W. Lehnert, J. Banhart, Applied Physics Letters 92, 244101 (2008)

[11] D. U. Sauer, T. Sanders, B. Fricke, T. Baumhöfer, K. Wippermann, A. A. Kulikovsky, H. Schmitz, J. Mergel, Journal of Power Sources 176 (2008) 477–483

[12] N. Kardjilov, A. Hilger, I. Manke, M. Strobl, W. Treimer, J. Banhart, Nuclear Instruments and Methods in Physics Research A 542 (2005) 16–21

[13] N. Akhtar, A. Qureshi, J. Scholta, C. Hartnig, M. Messerschmidt, W. Lehnert, International Journal of Hydrogen Energy 34 (2009) 3104–3111

[14] A. A. Kulikovsky, H. Schmitz, K. Wippermann, J. Mergel, B. Fricke, T. Sanders, D. U. Sauer, Electrochemistry Communications 8 (2006) 754–760
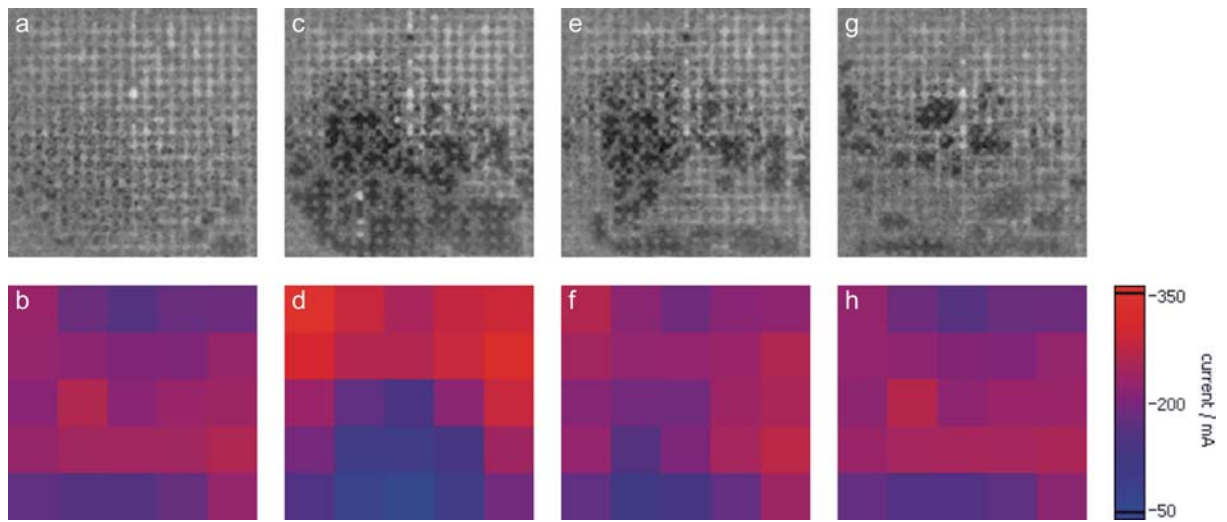
Fig. 1
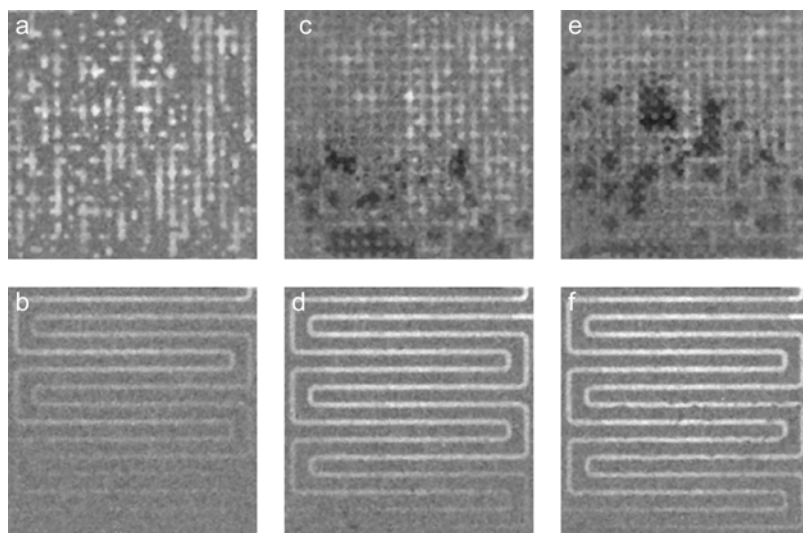
Fig. 2
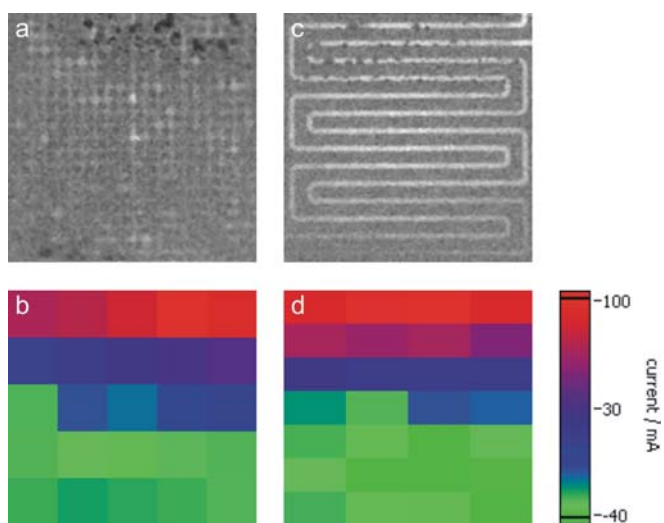
Fig. 3

Figure captions:

Fig. 1. Neutron radiographies and corresponding current distributions during flooding effect at 300 mA cm^{-2} average current density. Liquid water can be identified as dark spots along the bright channel area. a, b: t = 0 s; c, d: t = 270 s; e, f: t = 282 s;
g, h: t = 471 s (methanol flow rate: 2.19 ml min^{-1}, air flow rate: 378 ml min^{-1}).

Fig. 2. Comparison of water and gas distribution as function of current density in a grid structure and twofold meander flow field. a, b: 50 mA cm^{-2}; c, d: 150 mA cm^{-2};
e, f: 300 mA cm^{-2} (methanol flow rate: 2.19 ml min^{-1}, air flow rate: 378 ml min^{-1}).

Fig. 3. Neutron radiographies and corresponding current distributions during bi-functional operation; dark spots indicating liquid water can only be observed in the upper (galvanic) region of the electrochemically active area. a, b: grid flow field; c, d: twofold meander flow field (methanol flow rate: 2.56 ml min^{-1}, air flow rate: 20 ml min^{-1}).